COBEM 2021 26th International Congress of Mechanical Engineering
November 22-26, 2021, Virtual Congress, Brazil

COB-2021-1017
ELECTROCHEMICAL CORROSION RESISTANCE OF MARTENSITIC STAINLESS-STEEL COATINGS ON CARBON STEEL SUBSTRATES OBTAINED BY THERMAL SPRAYING AND FRICTION SURFACING

Gabriela de Andrade Oliveira
Carlos Roberto de Araújo
Fernanda Troysi
Pedro Brito
Pontifical Catholic University of Minas Gerais, Graduate Program in Mechanical Engineering (PPGEM), Av. Dom José Gaspar 500, Belo Horizonte (MG) 30535-901, Brazil.
gabiao26@hotmail.com, fernandadias.eng@outlook.com, carlosroberto_araujo@yahoo.com.br, pbrito@pucminas.br

Abstract. *Friction surfacing is a solid-state joining process that has been successfully applied for producing similar and dissimilar coatings of numerous metallic alloys, avoiding some of the problems associated with conventional fusion based welding techniques such as solidification cracking, formation of gas porosities and elevated residual stresses. In the present work, a comparison of the electrochemical corrosion resistance of AISI 420 martensitic stainless-steel coatings deposited on AISI 1045 carbon steel substrates by thermal spraying and friction surfacing is compared. The corrosion resistance was investigated by potentiodynamic polarization in 0.5M H_2SO_4 solution containing naturally dissolved O_2. The coatings were further analyzed in terms of mechanical properties (Vickers microhardness profiles determined along the materials cross sections) and microstructure. Both coatings exhibited similar hardness profiles, but it was possible to show that the coatings obtained by thermal spraying exhibited a relatively high level of porosities, which hindered its corrosion resistance compared to the coatings obtained by friction surfacing.*

Keywords: *Friction Surfacing; Thermal Spray; Coatings; Corrosion.*

1. INTRODUCTION

The AISI 1045 steel is widely used in numerous industrial sectors because of positive characteristics such as low cost, good weldability and machinability. In many applications, the material is exposed to hostile environments that can lead to premature failure or the manufactured components. As a result, there are several costings obtained by physical or chemical processes that combine corrosion resistance and wear.

One of these types of coatings is thermal spray coating process of ferrous alloys, which aims to protect surfaces against degradation at high temperature and wear, as well as to recompose parts sizing. Typical applications include thermal barriers with wear and corrosion resistance, high dielectric strength, dense and hard coating, etc. (Gedzevicius and Valiulis, 2006). Un thermal spraying, drops of the coating metal are sprayed into the surface to be coated at high speed. Although the process has high productivity, the solidification process of the coating can lead to the formation of continuity defects due to high cooling rates such as cracks or pores, in addition to the formation of diluted areas.

Recently, the friction surfacing (FS) process was developed, which allows the covering of metallic surfaces in solid state, seeking to avoid some of the problems associated with conventional coatings processes in which the materials involved are melted. The process was developed effectively from the beginning of the 1990s and has aroused growing interest from the scientific community since then, especially due to the growing demand for high performance coatings for applications considered critical (Gandra *et al*., 2014).

In the FS process, a rotating consumable rod is forced on the substrate to be coated. The friction between the surfaces causes the release of heat, the heating of the materials involved and intense plastic deformation at the tip pf the stem. As a consequence, a viscoplastic flow of the stem material is established, leading to the formation of the flash characteristic of the process. Then, the substrate translates into movement and the formation of a longitudinal deposit, with an aspect similar to a weld bead deposited on a plate. The main operational parameters are the axial force (F), the rotation speed (Ω) and the feed speed (Vx). Currently, it is considered that a possibility for exploring this type of process is its use in non-dedicated machinery such as, for example, in machining centers or milling machines (Vitanov *et al*., 2010; Gandra *et al*., 2014).

Among the techniques used to improve the performance of materials, deposition on the surface of components can be effective for the recovery of worn elements. With this, the need to select a stainless steel, for several industrial applications, with characteristics such as corrosion resistance of the alloy, mechanical properties, fabricability and cost,

for comparative study of its corrosion resistance in abrasive media, aiming at the production of lower cost parts, in comparison with solid parts of this steel (Casteletti, 2010).

2. EXPERIMENTAL PROCEDURE

The materials used in the present investigation were hot-rolled AISI 1045 medium carbon steel substrates and AISI 420 martensitic stainless steel, used for producing thermal spray and friction surfaced coatings. Before coating deposition, the materials were submitted to sandblasting for removing surface oxides. After surface cleaning, the thermal spray coatings were produced by using an electric arc TAFA 30 8B 35 equipment, with a stand-off distance of 250 mm, 1.6mm diameter AISI 420 steel wire, 35 A arc current, 30 V potential (Murilo *et al*., 2011).

The friction surfacing procedure was performed with the same materials as used in thermal spraying. The AISI 1045 steel substrate were used in the hot-rolled condition (200 x 100 x 8 mm sheets), while 15.4 x 100 mm circular bars were used for the AISI 420 coating material. The deposition parameters were 1500 rpm rotation, 190 mm/s, following optimization procedures performed in a previous investigation (Troysi *et al*., 2019).

The coatings produced by thermal spraying and friction surfacing were analysed in terms of microhardness and microstructure. Both analyses were performed along the cross section. The microhardness tests were performed using a Shimadzu HMV indenter, with 20 s load time and 0.025 gf load in conformity with the ASTM E384-17 standard and the microstructure was evaluated by optical microscopy following common metallography procedures (grinding in SiC and polishing in a diamond suspension down to a 1 µm finish.

Electrochemical tests for evaluating corrosion resistance were performed in a 0.5M H_2SO_4 solution containing naturally dissolved O_2. The samples were mounted in a flat cell with a 5 mm diameter orifice and a three-electrode setup was used. A 5 mm diameter platinum disc was used as counter-electrode while a Ag/Ag-Cl electrode served as reference electrode. The samples were first exposed to the selected electrolyte for 1 hour to allow for Open Circuit Potential (OCP) stabilization. Subsequently, potentiodynamic polarization scans were performed in the range of -0.6 to 2.0 V at a 0.2 mV/s scan rate, in similarity with previous investigations (Puli and Janaki Ram, 2012; Troysi and Brito, 2020). All tests were performed three times to ensure reproducibility. Finally, in order to elucidate corrosion mechanisms, the friction surfaced coatings were analysed by Electrochemical Impedance Spectroscopy (EIS) at the stabilized OCP by applying a 0.01V amplitude sinusoidal signal at frequencies of 100,000 to 0.01 Hz.

3. RESULTS AND DISCUSSION

3.1. COATING DEPOSITION AND PROPERTIES

An overview of the coating deposition process by friction surfacing is presented in Figure 1. In Figure 1(a), the main process parameters are identified: rotation (R) and forward speed (V). The process begins with downward motion of the rotating consumable rod. As shown in Figure 1(b), friction between the contact surfaces generates heat and the temperature at the interface rises. Downward motion continues until the material located at the rod tip undergoes plastic deformation generating flash, as shown in Figure 1(c). Then, forward motion is imposed on the rod which allows the formation of a continuous deposit, Figure 1(d).

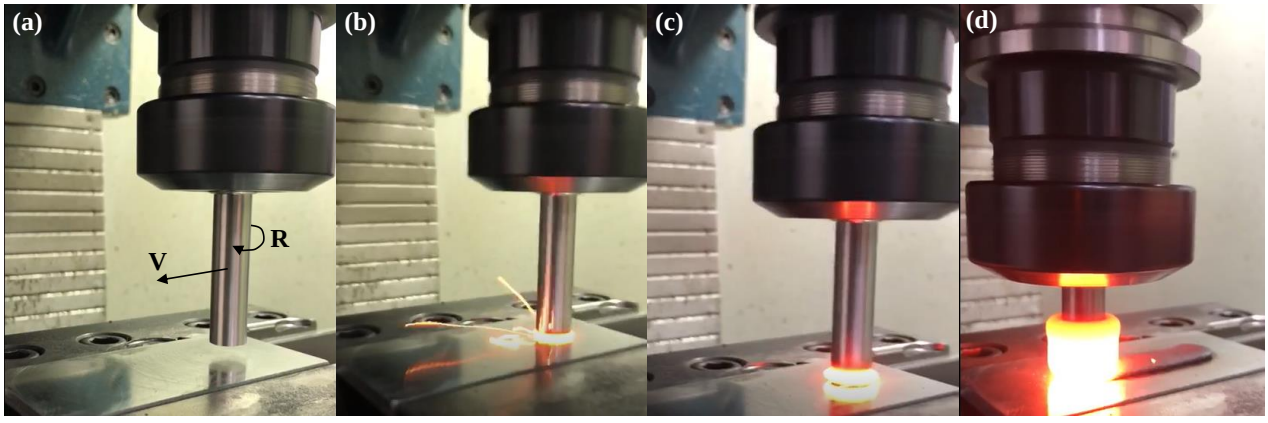

Figure 1. Coating deposition by friction surfacing: (a) pre-contact setup, (b) initial contact, (c) flash formation at the consumable rod tip and (d) coating deposition.

The characteristics of the coating/substrate interfaces of the friction surfaced and thermal sprayed coatings are compared in Figure 2(a) and 2(b), respectively, while the microhardness depth profiles for both coatings are presented in Figure 3. In Figure 2, it is possible to observe a continuous interface for both coating systems. The coating produced by thermal spraying presented several pores, indicated by arrows in Figure 2(b), which are caused by the rapid solidification

process and insufficient wetting during deposition. These defects were not present in the friction surfaced coating, as can be seen in Figure 2(a) because the process takes place in the solid state. Concerning the results presented in Figure 3, it is possible to see that both coatings exhibited elevated hardness values (> 500 HV). The friction surfaced coating presented, however, a more homogenous hardness distribution within the coating (567 ± 18 HV) compared to the thermal sprayed coating (473 ± 37 HV), suggesting superior uniformity of the coating produced in the solid state, as well as the negative impact of porosities formed in the thermal sprayed coating. In particular, the thermal sprayed coating exhibited a significant hardness loss close to the surface in comparison to the regions near the interface with the substrate steel.

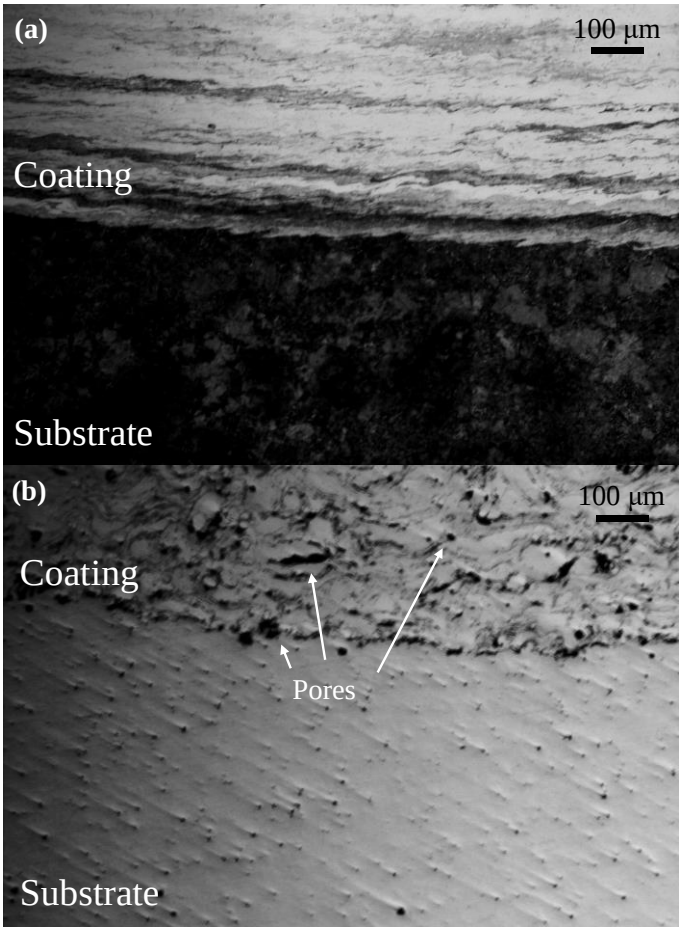

Figure 2. Interface characteristics of friction surfaced (a) and thermal sprayed (b) coatings.

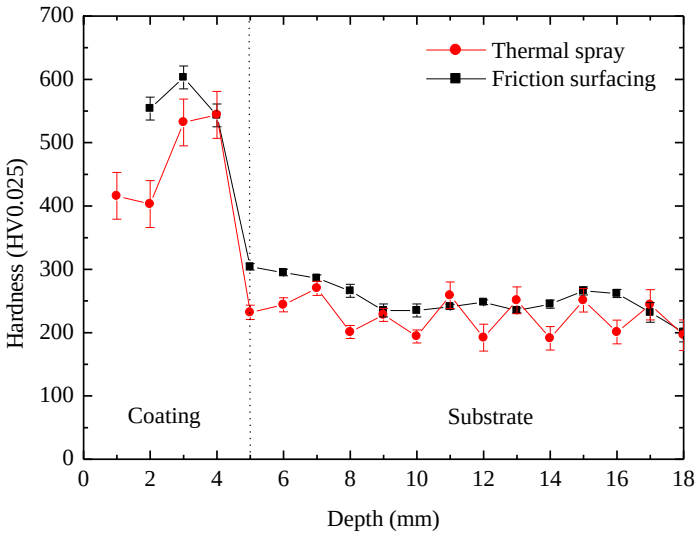

Figure 3. Vickers microhardness variation along the cross section of thermal sprayed and friction surfaced coatings.

3.2. CORROSION RESISTANCE

The results showing OCP stabilization of the thermal sprayed and friction surfaced coatings in 0.5M H_2SO_4 containing naturally dissolved O_2 are presented in Figure 4 (the most representative of three measurements performed on each sample condition are presented). In both cases, after 3600 s exposition, variations of electrode potential were smaller than 10 mV/hour and were considered stable. It is possible to notice that the final stabilized value observed for both coatings indicates less reactive (less negative) behaviour for the friction surfaced coating relative to the thermal sprayed coating.

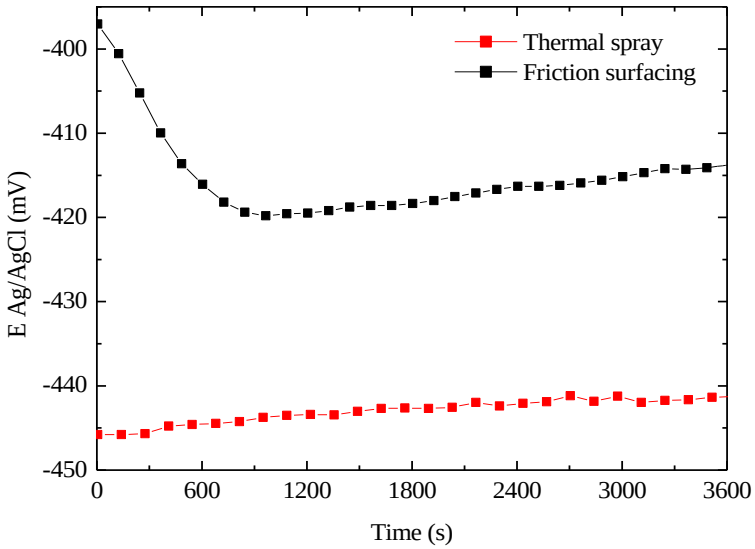

Figure 4. OCP stabilization of the thermal sprayed and friction surfaced coatings in 0.5M H_2SO_4 containing naturally dissolved O_2.

After OCP stabilization, potentiodynamic polarization scans were performed. The resulting polarization diagrams are presented in Figure 5 and the data obtained are summarized in Table 1. The results show that both coatings exhibit an active/passive transition, but significantly different characteristics in both active and passive behaviours. The active behaviour is described by the corrosion current density (i_{corr}), which is a measure of the corrosion rate in the absence of a passive layer, and the corrosion potential (E_{corr}). These parameters were obtained from the polarization curves by modelling the active region with the Butler-Volmer equations (McCafferty, 2010):

$$i = i_{\text{corr}}\left[e^{\frac{2.303(E-E_{\text{corr}})}{b_C}} - e^{\frac{2.303(E-E_{\text{corr}})}{b_A}}\right] \quad (1)$$

where b_C and b_A are the cathodic and anodic slopes, respectively. An example of the experimental data fitted to equation (1) is presented in Figure 6.

Concerning the active corrosion behaviour, the friction surfaced coatings exhibited superior resistance with lower values of i_{corr} and more noble values for E_{corr}, on average, as show in Table 1. It is important to consider, however, that in a real application in which a passive layer is present on the metal surface, the corrosion resistance must also take into account the passivation characteristics of the material.

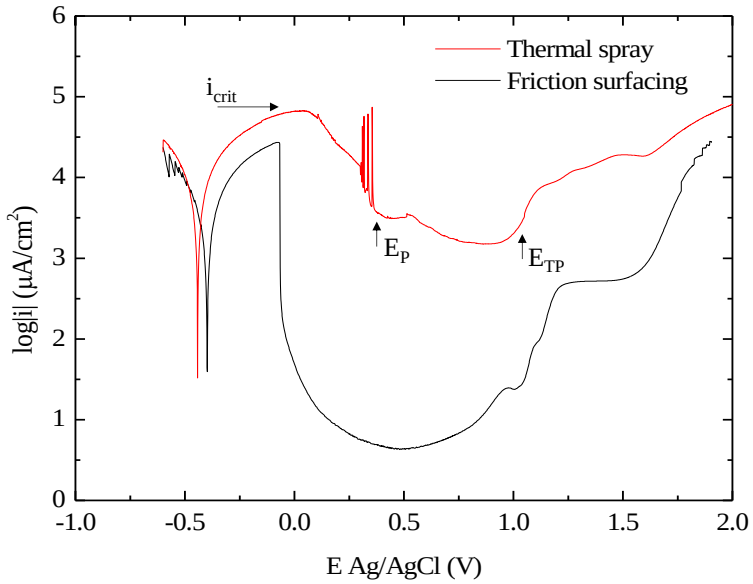

Figure 5. Potentiodynamic polarization scans performed on the thermal sprayed and friction surfaced coatings in 0.5M H_2SO_4 containing naturally dissolved O_2.

Table 1. Summary of potentiodynamic polarization results obtained from the thermal sprayed (TS) and friction surfaced (FS) coatings in 0.5M H_2SO_4 containing naturally dissolved O_2 (i_{corr}: corrosion current density, E_{corr}: corrosion potential, i_{crit}: critical corrosion density, ΔE_{pass}: passivity range, i_{pass}: passive current density).

Sample	i_{corr} (mA/cm^2)	E_{corr} (V)	i_{crit} (mA/cm^2)	ΔE_{pass} (V)	i_{pass} (μA/cm^2)
TS	20.8 ± 2.49	-0.44 ± 0.010	64.8 ± 5.06	0.54 ± 0.04	429 ± 55.3
FS	2.57 ± 2.00	-0.39 ± 0.007	24.3 ± 4.7	1.07 ± 0.09	2.24 ± 0.97

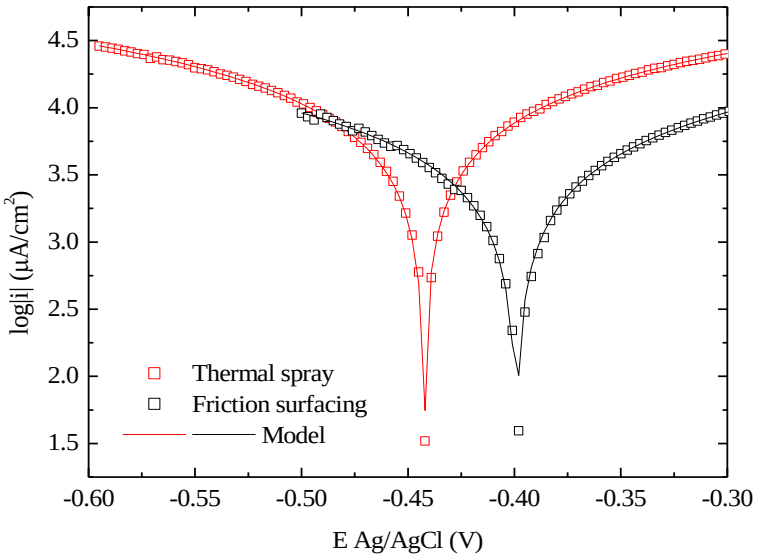

Figure 6. Butler-Volmer model analysis (active corrosion) of thermal sprayed and friction surfaced coatings in 0.5 M H_2SO_4 containing naturally dissolved O_2.

With regards to the passive corrosion behaviour, the obtained results also show superior behaviour of the friction surfaced coating when compared to the coating obtained by thermal spraying. First, the critical current density (i_{crit}), is lower for the friction surfaced coating which means that a lower quantity of metal is dissolved prior to the formation of the passive layer. The passivity range (ΔE_{pass}) in the present investigation was determined by the difference between the passivation potential (E_P) and the transpassive potential (E_{TP}), which are both identified in Figure 5. The passive current density (i_{pass}), which determines the actual corrosion rate in the presence of a passive layer was calculated as the average

value of current density between E_P and E_{TP}. Both parameters, i_{pass} and ΔE_{pass}, indicate that a more stable passive layer was developed on the friction surfaced coating when compared to the coating obtained by thermal spraying.

This behaviour is probably connected with the presence of pores in the coating obtained by thermal spray, which could lead to infiltration of the electrolyte in the coating. Since the medium carbon steel substrate is significantly more anodic compared to the stainless-steel coating, the corrosion rate would be expected to increase significantly with the formation of a galvanic pair between coating and substrate. It is also possible to consider that chemical heterogeneities are present in the thermal spray coating, as suggested by the variations in microhardness observed towards the outer coating surface.

3.3 ELECTROCHEMICAL IMPEDANCE SPECTROSCOPY (EIS) ANALYSIS

An analysis of the corrosion mechanisms involved in the exposure of the friction surfaced coatings to the 0.5 M H_2SO_4 solution was performed by applying EIS, and the results are presented in Figure 7. The experimental data were fitted against the equivalent circuit model shown in the inset of Figure 7, which represents a simple electrochemical interface formed by an electrical double layer (McCafferty, 2010). The electrical double layer is composed of the polarization resistance R_P and a capacitive element C_{DL}, while the term R_S represents the ohmic resistance of the electrolyte.

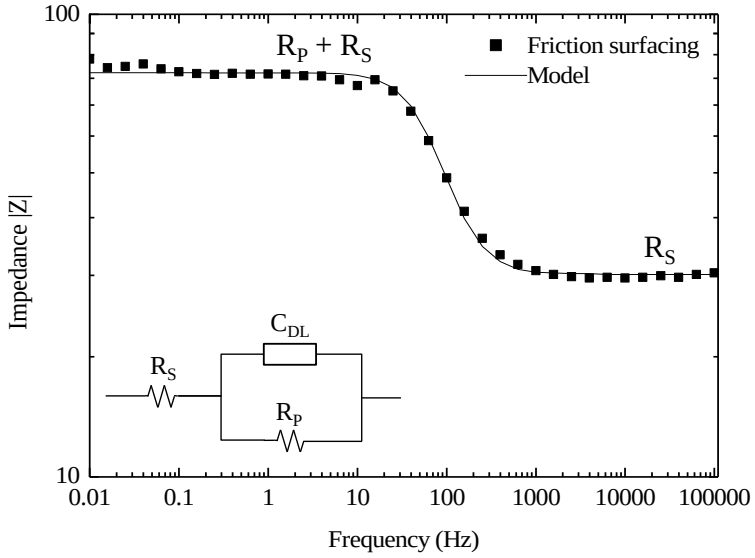

Figure 7. EIS results (Bode diagram) obtained from the thermal sprayed and friction surfaced coatings in 0.5 M H_2SO_4 containing naturally dissolved O_2

Table 2. Summary of the EIS data obtained friction surfaced (FS) coatings in 0.5M H_2SO_4 containing naturally dissolved O_2. Error values for each parameter are given in parenthesis (R_S: solution impedance, R_P: polarization resistance, C_{DL}: double layer capacitance).

Sample	R_S (Ω)	R_P (Ω)	C_{DL} (F)
FS	27.4 (0.54%)	47.3 (0.79%)	5.86×10^{-5} (2.11%)

For equivalent circuit presented in Figure 7, the absolute impedance value |Z| is given by (McCafferty, 2010):

$$|Z| = \left[\left(R_S + \frac{R_P}{1+\omega^2 {R_P}^2 {C_{DL}}^2}\right)^2 + \left(\frac{\omega {R_P}^2 C_{DL}}{1+\omega^2 {R_P}^2 {C_{DL}}^2}\right)^2\right]^{1/2} \quad (2)$$

The analysis shows that for very low frequency values, the total absolute impedance value becomes equal to R_S + R_P while at very high frequencies, the absolute impedance becomes equal to R_S. The experimental data fitted to the simple electrical double layer model, which indicates that a single time constant is present at the electrochemical interface formed by the outer coating surface and the electrolyte. This is an indirect indication that the coating formed by friction surfacing is continuous and is not permeated by the electrolyte.

4. CONCLUSIONS

In the present work, the corrosion resistance of thermal sprayed and friction surfaced coatings of AISI 420 martensitic stainless-steel coatings deposited on AISI 1045 carbon steel substrates was compared. The thermal sprayed coating exhibited a relatively high number of pores as well as hardness variations which suggest chemical heterogeneity. Overall, the friction surfaced coatings exhibited superior corrosion resistance regarding both active (lower values of corrosion rate and less reactive corrosion potential) and passive behaviors (lower value of dissolution rate and larger passivity range). Finally, EIS analysis of the friction surfaced coating indicated the formation of a simple electrochemical interface, corresponding to a continuous and impermeable coating.

5. ACKNOWLEDGEMENTS

The authors acknowledge financial support from CNPq (grant numbers 444864/2020-2 and 315533/2020-0) and FAPEMIG (grant number PPM-00662-18). Mr. Ítalo Bruno dos Santos is acknowledge for assistance in producing the friction surfaced coatings.

6. REFERENCES

Castelett, L. C., 2010. “Avaliação da resistência à corrosão do aço AISI 420 depositado por processos variados de aspersão térmica”. *Revista Esola de Minas*, Vol. 63, No. 1, pp. 87-90.

Gandra, J., Krohn, H., Miranda, R. M., Vilaça, P., Quintino, L., dos Santos, J. F., 2014. “Friction Surfacing – A Review”, *Journal of Materials Processing Technology*, Vol. 214, pp. 1062-1093.

Gedzevicius, I., Valiulis, A. V., 2006. “Analysis of wire arc spraying process variables on coatings properties”, *Journal of Materials Processing Technology*, Vol. 175, No. 1-3, pp 206–211.

Murilo, N. A., Carneiro, J. R. G., Branco, J. R. T., Costa, L. V., Lourenço, M. M., 2011. “Estudo da Adesão e desgaste de recobrimento por aspersão térmica a arco duplo arame de aço AISI 420 em substrato ABNT 1045”, in: An. Do 6º Congr. Bras. Eng. Fabr., Associação Brasileira de Ciências Mecânicas (ABCM), Caxias do Sul, pp. 1–10.

McCafferty, E., 2010. *Introduction to corrosion science*. Springer Science & Business Media, 2010.

Puli, R., Janaki Ram, G. D., 2012. “Corrosion performance of AISI 316L friction surfaced coatings”, *Corrosion Science*, Vol. 62, pp. 95-103.

Troysi, F., Silva, K., dos Santos, Í., Brito, P., 2019. “Investigation of austenitic stainless steel coatings on mild steel produced by friction surfacing using a conventional CNC machining center”, *Materials Research*, Vol. 22, No. 2, pp. e20180301.

Troysi, F., Brito, P., 2020. “Development and characterization of an iron aluminide coating on mild steel substrate obtained by friction surfacing and heat treatment”, *The International Journal of Advanced Manufacturing Technology*, Vol. 111, No. 9, pp. 2569-2576.

Stoynov, Z., 1990. “Impedance modeling and data processing: structural and parametrical estimation”, *Electrochimica Acta*, Vol. 35, pp. 1493-1499.

Vitanov, V. I., Javaid, N., Stephenson, D. J., 2010. “Application of Response Surface Methodology for the optimization of Micro Friction Surfacing Process”, *Surface and Coatings Technology*, Vol. 204, No. 21-22, pp. 3501-3508.

7. RESPONSIBILITY NOTICE

The authors are the only responsible for the printed material included in this paper.